ce/papers Proceedings in civil engineering
eurosteel CRACOW 2026
WILEY

Full paper

Laser Scanning-based Assessment of Geometrical Imperfections in Welded I-sections with Varying Flange Fabrication Processes

Dénes Kollár[1] | András Horváth[1] | Balázs Kövesdi[1] | Maxime Lebastard[2] | Alain Bureau[2]

Correspondence

Dr. Dénes Kollár
Budapest University of Technology and Economics
Department of Structural Engineering
3 Műegyetem rkp.
1111 Budapest, Hungary
Email: kollar.denes@emk.bme.hu

[1] Budapest University of Technology and Economics, Faculty of Civil Engineering, Department of Structural Engineering, Budapest, Hungary
[2] Centre Technique Industriel de la Construction Métallique, Saint-Aubin, France

Abstract

Accurate characterization of geometrical imperfections in welded members is essential for structural design and for calibrating advanced numerical models. This study presents a detailed investigation of imperfections in a total of thirteen welded I-sections using a 3D laser scanner. The studied members comprise plasma-cut, flame-cut and hot-rolled flanges with varying cross-sectional dimensions. The resulting point clouds are processed in MATLAB, where filtering and smoothing techniques are applied to quantify imperfections in accordance with EN 1090-2. The evaluation covers global bow imperfections about both major and minor axes, out-of-straightness, out-of-squareness, flange flatness and distortion, as well as local web imperfections. Results indicate that global bow imperfections about the major axis generally remain within the EN 1090-2 tolerance of $L/1000$. Conversely, bow imperfections about the minor axis frequently exceed manufacturing tolerances, particularly in specimens with flame-cut flanges, where welding-induced shrinkage has a pronounced influence. Local flange imperfections, combining the effects of assembly errors and welding distortions, can vary between $b_f/85$ and $b_f/500$ based on the current measurements, surpassing even the recommended amplitudes for advanced finite element analysis with equivalent geometrical imperfections. Web distortions range from $h_w/545$ to $h_w/103$, exceeding code-based essential tolerances in four specimens. These findings highlight that imperfections arising from welding and flange fabrication processes often exceed recommended design values, suggesting that existing geometrical imperfection recommendations in EN 1993-1-14 may require reassessment for realistic implementation in advanced finite element-based structural analyses.

Keywords

I-section, Geometrical imperfection, Welding, Plasma-cut flanges, Flame-cut flanges, Hot-rolled flanges

1 Introduction

Accurate characterization of residual stresses and geometrical imperfections in welded members is essential for structural design and for calibrating advanced numerical models. Several studies have reported geometric imperfections in welded I-sections, mainly focusing separately on local plate imperfections or global bow imperfections. Xu et al. [1] measured local flange and web imperfections in sixteen welded stub columns, reporting flange imperfection magnitudes in the range of $b_f/209$ to $b_f/35$ (14 out of 16 specimens exceeding the functional tolerances in EN 1090-2 for class 2) and web imperfections between $h_w/1992$ and $h_w/175$, where b_f and h_w denote flange width and web height, respectively. Yun et al. [2] investigated five high-strength (S690) and hybrid steel (S355+S690) columns and documented in-plane global bow imperfections with magnitudes of $L/2597$ to $L/1818$, where L is the specimen length. Su et al. [3] examined ten S960 welded stub columns and found maximum local plate imperfections varying from $h_w/2000$ to $h_w/1091$. Lebastard et al. [4] reported global bow imperfections in four tapered and uniform S355 normal strength steel beams, with magnitudes between $L/1911$ and $L/1263$, while local web plate imperfections varying between $h_w/584$ and $h_w/214$. Nascimento et al. [5] measured local web plate imperfections in eight stiffened I-sections from S355 structural steel grade, identifying magnitudes ranging from $h_w/155$ to $h_w/70$ (7 out of 8 specimens not fulfilling the functional tolerances in EN 1090-2). In addition, Tankova [6] documented in-plane ($L/4615$-$L/2857$) and out-of-plane ($L/2857$-$L/1333$) global bow imperfections for three non-uniform specimens with non-parallel flanges. Moreover, Schaper et al. [7] reported in-plane ($L/5350$-$L/828$, 1 out of 8 I-sections exceeding the functional tolerances specified for class 2 in EN 1090-2) and out-of-plane ($L/12126$-$L/2125$) global bow imperfections

https://doi.org/10.1002/cepa.70311

along with initial twist rotations (8.1-25.9 mrad).

Previous measurements have not explicitly examined how flange fabrication influences geometrical imperfections. This paper addresses that gap by studying the impact of plasma cutting, flame cutting, and hot rolling on geometrical imperfections in welded I-section members. To provide the necessary experimental evidence, an extensive shape-measurement programme is carried out on welded I-sections with various flange fabrication methods and cross-sectional sizes.

2 Experimental programme

A comprehensive experimental programme is conducted on a total of fifteen welded I-sections (**Table 1**) manufactured from S355 structural steel grade. The programme focuses on (i) measuring cross-sectional dimensions, (ii) determining mechanical properties using tensile tests (measured yield strength f_y and ultimate strength f_u varying between 334-411 MPa and 525-546 MPa, respectively), (iii) residual stress measurements applying both sectioning technique and contour method, and (iv) shape measurements for evaluating initial geometrical imperfections due to fabrication. Details of the experimental programme can be found in [8]. In general, the background and results of the shape measurements are presented hereafter.

Table 1 Measured average cross-sectional dimensions of I-section members included in initial geometrical imperfection measurements

Flange	Specimen	h_w [mm]	t_w [mm]	b_f [mm]	t_f [mm]	L [m]
Plasma-cut	WPC_6_2.5_12	598.5	6.1	249.5	12.1	2.5
	WPC_6_1.5_20	598.0	5.9	151.0	20.2	2.5
	WPC_6_3_20	600.0	5.9	300.5	20.1	2.5
	WPC_6_1.5_12	600.0	6.3	150.5	12.1	2.5
	WPC_4_1.2_15	399.0	6.2	121.0	15.2	2
	WPC_4_1.5_12	397.0	6.1	150.0	12.1	2
	WPC_6_1.5_12/20	600.0	6.2	150.0	20.1$^{(1)}$ 12.1$^{(2)}$	2.5
	WPC_4_2_20	398.5	6.3	201.0	20.2	2
Flame-cut	WFC_6_1.5_20_235	598.0	5.9	151.0	20.1	2.5
	WFC_6_1.5_20	601.0	6.2	149.0	20.2	2.5
	WFC_6_1.7_12	600.0	6.1	169.5	20.2	2.5
	WFC_4_1.5_12	397.5	6.1	150.0	12.1	2
	WFC_4_1.2_12	398.0	6.2	119.0	12.2	2
Hot-rolled	WHR_6_1.5_20	599.5	6.1	147.5	20.2	2.5
	WHR_4_1.5_12	398.0	6.1	150.5	12.1	2

Note: (1) and (2) denotes that a mono-symmetric I-section is tested with different top and bottom flange thicknesses.

Shape measurements are performed using the Scantech KSCAN-Magic handheld three-dimensional (3D) laser scanner, which employs non-contact measurement technology, with a scanning accuracy of up to 0.020 mm and a resolution of up to 0.010 mm. Reference targets, i.e., small circular markers, are installed on the specimens (**Figure 1**) to precisely determine their location on the measured surfaces and serve as control points. The shape of thirteen out of the total fifteen specimens is measured, while specimens WFC_4_1.2_12 and WPC_4_2_20 have been cut into two parts prior to shape measurements in order to determine residual stresses by using the sectioning technique. Consequently, no shape measurements were performed for these two specimens.

3 Measurement results

The measured point clouds are assessed in MATLAB [9]. The relevant geometrical imperfection components (**Figure 2**) of the welded I-sections, in accordance with Annex B of EN 1090-2 [10], are determined after filtering and smoothing. Imperfection types and the corresponding manufacturing tolerances are summarized in **Table 2**. Essential tolerances define the basic limits required to satisfy the design assumptions for structural resistance and stability. Functional tolerances, which may be needed to meet appearance or fit-up requirements, are also listed in the table for tolerance classes 1 and 2, where applicable. In general, tolerance class 1 applies unless otherwise specified in the execution specification, in accordance with the standard. It is underscored that geometrical imperfections presented hereafter include the effect of all the manufacturing steps, e.g., out-of-flatness of constituent plates due to hot-rolling, assembly errors such as out-of-squareness of flanges or web eccentricity, welding-induced distortions, etc.

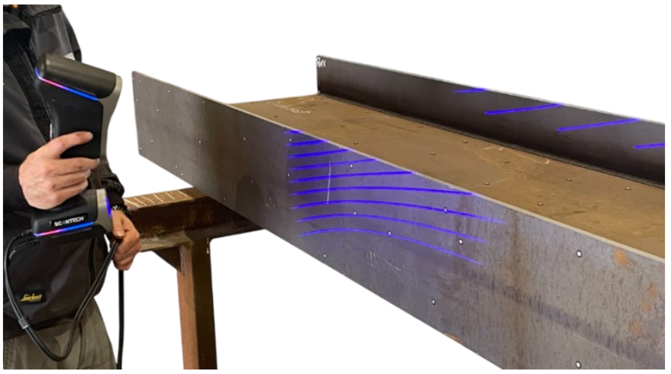

Figure 1 I-section with reference targets during laser scanning

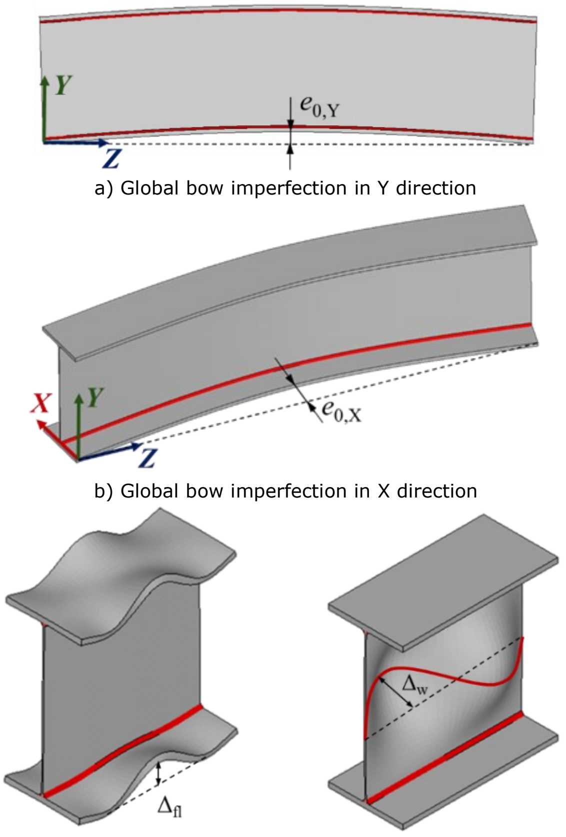

Figure 2 Typical geometrical imperfections of the measured I-sections

Table 2 Relevant manufacturing tolerances for welded I-sections according to the tables in Annex B of EN 1090-2 (reference dimensions are denoted by L, b and t) including the main causes during manufacturing

Criterion (Main cause)	Permitted deviation Δ: Essential tolerances	Permitted deviation Δ: Functional tolerances	
	Class 1 and 2	Class 1	Class 2
Out-of-straightness, Table B.6 (Eccentric welds)	No requirement	$\pm L/1000$, but $\lvert\Delta\rvert \geq 5$ mm	$\pm L/1000$, but $\lvert\Delta\rvert \geq 3$ mm
Out-of-squareness, Table B.1 (Assembly error)	No requirement	$\pm b/100$, but $\lvert\Delta\rvert \geq 5$ mm (general case)	$\pm b/100$, but $\lvert\Delta\rvert \geq 3$ mm (general case)
Out-of-flatness, Table B.1 (Welding-induced angular distortion)	No requirement	$\pm b/150$, but $\lvert\Delta\rvert \geq 3$ mm (general case)	$\pm b/150$, but $\lvert\Delta\rvert \geq 2$ mm (general case)
Flange distortion, Table B.3 (Initial shape of plate + welding-induced local buckling)	$\pm b/150$ if $b/t \leq 20$, $\pm b^2/(3000t)$ if $b/t > 20$	$\pm b/100$	$\pm b/150$
Plate curvature & Web distortion, Table B.1 (Initial shape of plate + welding-induced local buckling)	Plate curvature: $\pm b/200$ if $b/t \leq 80$), $\pm b^2/(16000t)$ if $80 \leq b/t \leq 200$, $\pm b/80$ if $b/t > 200$, but $\lvert\Delta\rvert \geq t$ Web distortion: $\pm b/100$, but $\lvert\Delta\rvert \geq t$	$\pm b/100$, but $\lvert\Delta\rvert \geq 5$ mm	$\pm b/150$, but $\lvert\Delta\rvert \geq 3$ mm

Firstly, magnitudes of out-of-straightness about both minor and major axes are evaluated. Thin-plate smoothing spline is applied to the data points representing the outer surface of the flanges. Then, points along the flanges, representing the intersection with the web, are plotted over the entire length to evaluate out-of-straightness about the major axis (i.e., global bow imperfection about the major axis in the Y direction) for each specimen (**Figure 3a**). The magnitudes, denoted as $e_{0,major}$, are ranging from 0.4 mm to 2.2 mm corresponding to $L/6250$ to $L/1136$ depending on the length L of each I-section. Thus, bow imperfection of all specimens in the Y direction fulfil the requirement ($L/1000$) of EN 1090-2. The total maximum value is $L/1136$, which is slightly smaller than the recommended amplitude in EN 1993-1-14 [11] (80% of the corresponding manufacturing tolerance, but at least $L/1000$) for advanced finite element analysis incorporating both geometrical and structural imperfections.

On the other hand, Savitzky-Golay filtering is applied to evaluate the distorted shapes of lower (**Figure 3b**) and upper flanges (**Figure 3c**) in the X direction in accordance with **Figure 2**. Out-of-straightness about the minor axis $e_{0,minor}$ (i.e., global bow imperfection about the minor axis in the X direction), primarily due to welding-induced longitudinal shrinkage and eccentricity of weld beads, are varying between 0.1 mm and 4 mm, which are $L/25000$ and $L/625$, respectively. Therefore, the tolerance of $L/1000$ is not met for the bow imperfection in the X direction for three welded specimens with flame-cut flanges (WFC_6_1.5_20_235, WFC_6_1.5_20, and WFC_4_1.5_12).

Secondly, amplitudes of out-of-squareness and out-of-flatness of the flanges (in conjunction with flange distortion, if any) could not be distinctly separated in the measured data point. These deviations mainly represent the combined effect of assembly error (during tack welding) and welding-induced angular distortion. The global shape of the flanges $U_{Y,global}(Z)$ used for determining $e_{0,major}$ at the flange-web intersection (**Figure 4a**) is extended in the width direction (X direction), resulting in $U_{Y,global}(X,Z)$ as shown in **Figure 4b**. The contribution of local imperfections **Figure 4c**) is then obtained by computing the devia-

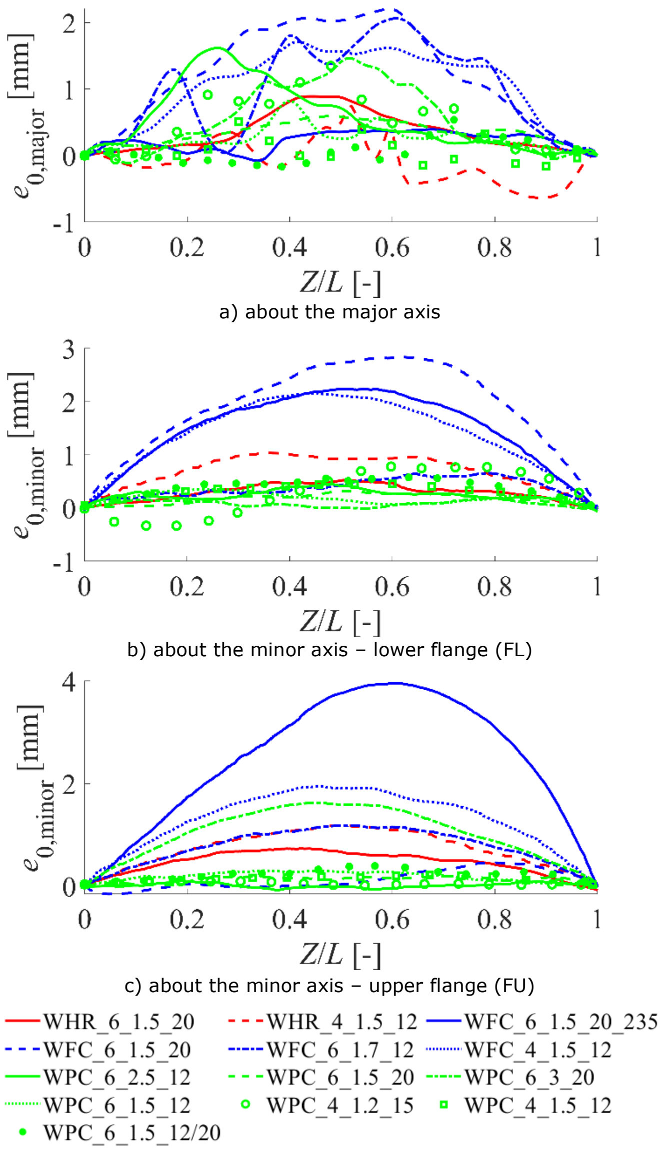

Figure 3 Measured out-of-straightness profiles for each I-section

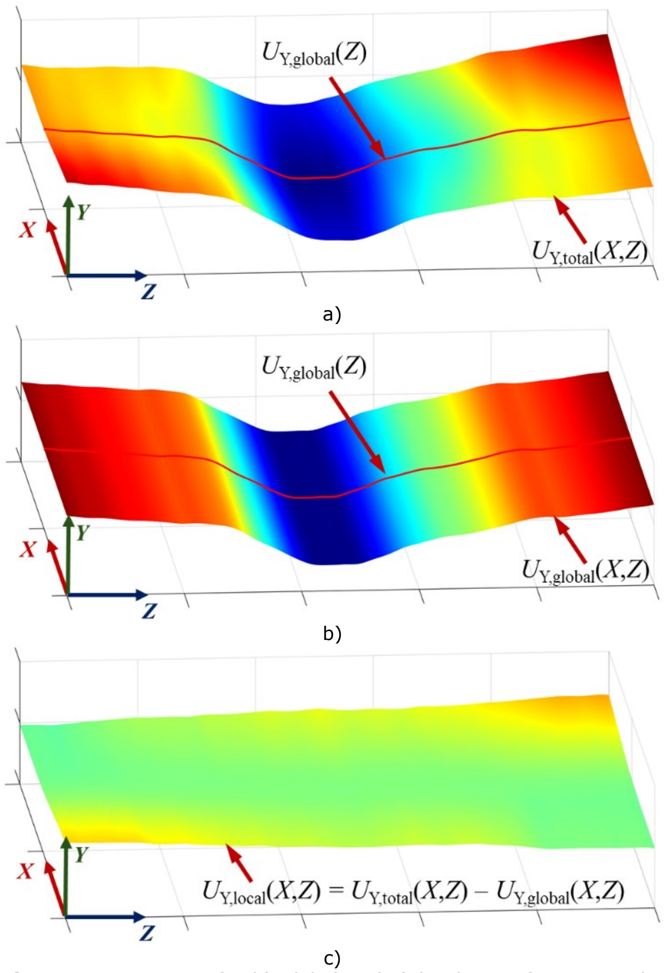

Figure 4 Derivation of a-b) global and c) local imperfections in the flanges from total measured shape

tion of the total shape $U_{Y,total}(X,Z)$ from the global shape $U_{Y,global}(X,Z)$, expressed as $U_{Y,local}(X,Z) = U_{Y,total}(X,Z) - U_{Y,global}(X,Z)$.

Magnitudes of local imperfections in the flanges Δ_{fl}, as the sum of previously mentioned phenomena, are varying between 0.3 mm and 2.5 mm, which are $b_f/500$ and $b_f/85$, respectively. It is noteworthy that equivalent local geometrical imperfection, incorporating the influence of residual stresses and geometrical imperfection, for flanges is $b_f/2/200 = b_f/400$ in EN 1993-1-14 in the case of local buckling-type imperfection, which is surpassed by 11 out of 13 specimens. On the other hand, it is $b_f/2/50 = b_f/100$ based on angular distortion or twist in the design standard. The overall maximum in the measured specimens, namely $b_f/85$, is larger than both values in the design codes for advanced finite element analysis, while not surpassing the $b_f/100 + b_f/150 = b_f/60$ magnitude for the combination of out-of-squareness and out-of-flatness in accordance with EN 1090-2. It suggests that these imperfection amplitudes in the design codes need to be reassessed for practical application in finite element method-based design incorporating both geometrical and structural imperfections. Local buckling-type imperfection, i.e., flange distortion, could be only identified in two specimens, namely WFC_6_1.5_20_235 and WPC_6_3_20.

Local imperfections, such as plate curvature and distortion of the web, are evaluated as well after using thin-plate smoothing spline for data points (using $U_{Y,local}$ data). Amplitudes Δ_w are varying between 1.1 mm and 5.8 mm, which are $h_w/545$ and $h_w/103$, respectively. In 5 out of 13 specimens, local geometrical imperfections in the web exceed the amplitude of $h_w/200$ denoting the recommended equivalent local geometrical imperfection in EN 1993-1-14. On the other hand, local imperfection of the web is larger than the essential tolerance as per EN 1090-2 ($h_w/200$ for $h_w/t_w = 400/6 = 66.7$ and $h_w/160$ for $h_w/t_w = 600/6 = 100$) for 4 out of 13 specimens. Exceedance of local flange and web imperfection tolerances seem unaffected by the flange fabrication process, though further data are required for clarification. Nevertheless, similarly to the equivalent geometrical imperfection corresponding to the flange, it is suggested that reassessing the amplitude in the design codes is reasonable for practical application in finite element method-based design. Evaluated local imperfections for lower (FL) and upper flange (FL), and the web plate (W) are plotted for specimen WPC_6_1.5_12/20 in **Figure 5** as an example. Measured magnitudes of the aforementioned geometrical imperfections are summarized in **Table 3** for all the specimens.

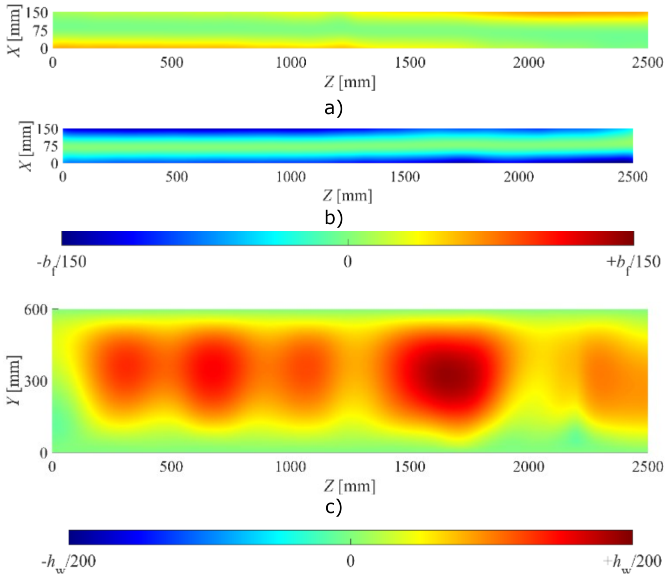

Figure 5 Measured local imperfections: a) Δ_{fl} in lower flange (FL), b) Δ_{fl} in upper flange (FU), and c) in web plate (W) for specimen WPC_6_1.5_12/20

4 Conclusions

Based on the initial geometrical imperfection measurements, the following conclusions could be drawn regarding welded I-sections with varying flange fabrication processes:

- out-of-straightness about the major axis for all specimens, regardless of flange fabrication method, satisfies the limit of $L/1000$ in EN 1090-2;
- out-of-straightness about the minor axis of three flame-cut welded I-section members does not fulfil the requirement of relevant manufacturing tolerances;
- welded I-section members with plasma-cut flanges exhibit the lowest out-of-straightness magnitudes ($L/25000$-$L/1563$);
- local flange imperfections—primarily resulting from welding-induced angular distortion and out-of-squareness during assembly—exceed the $b_f/150$ manufacturing tolerance in 11 of the 13 specimens;
- local imperfection of the web is larger than the essential tolerance as per EN 1090-2 for 4 out of 13 I-section members (specimens with plasma-cut and flame-cut flanges);

Table 3 Summary of shape measurements of welded I-girders (imperfections exceeding the essential tolerances or functional tolerances for tolerance class 1, as specified in EN 1090-2, are highlighted in bold letters)

Flange	Specimen	$e_{0,major}$ [mm]	$e_{0,minor}$ [mm] FL	FU	Δ_w [mm]	Δ_{fl} [mm] FL	FU	$L/e_{0,major}$ [-]	$L/e_{0,minor}$ [-] FL	FU	h_w/Δ_w [-]	b_f/Δ_{fl} [-] FL	FU
Plasma-cut	WPC_6_2.5_12	1.6	0.5	0.1	5.8	2.5	2.1	1563	5000	25000	**103**	**100**	**119**
	WPC_6_1.5_20	0.6	0.3	0.2	1.1	0.7	0.6	4167	8333	12500	545	214	250
	WPC_6_3_20	1.5	0.2	1.6	5.8	1.0	1.0	1667	12500	1563	**103**	300	300
	WPC_6_1.5_12	0.8	0.4	0.3	3.3	1.1	1.2	3125	6250	8333	182	**136**	**125**
	WPC_4_1.2_15	1.3	0.8	0.1	1.9	0.5	0.4	1538	2500	20000	211	240	300
	WPC_4_1.5_12	0.5	0.5	0.2	1.3	1.0	1.2	4000	4000	10000	308	**150**	**125**
	WPC_6_1.5_12/20	0.5	0.6	0.4	2.9	0.5	1.1	5000	4167	6250	207	300	**136**
	WPC_4_2_20*												
Flame-cut	WFC_6_1.5_20_235	0.4	2.2	4.0	1.3	0.5	0.7	6250	1136	**625**	462	300	214
	WFC_6_1.5_20	2.2	2.8	0.5	3.9	0.4	0.4	1136	**893**	5000	**154**	375	375
	WFC_6_1.7_12	2.1	0.7	1.2	4.4	2.0	1.5	1190	3571	2083	**136**	**85**	**113**
	WFC_4_1.5_12	1.7	2.2	1.9	1.2	1.2	1.3	1176	**909**	1053	333	**125**	**115**
	WFC_4_1.2_12*												
Hot-rolled	WHR_6_1.5_20	0.9	0.5	0.7	1.5	0.3	0.4	2778	5000	3571	400	500	375
	WHR_4_1.5_12	0.7	1.0	1.2	1.4	1.0	1.0	2857	2000	1667	286	**150**	**150**

Note: *Specimens have been cut into two parts prior to shape measurements in order to determine residual stresses by using the sectioning technique.

- imperfection amplitudes in design codes may require reconsideration for finite element method-based design, with particular attention to differentiating the effects of flange fabrication process.

Acknowledgement

The presented paper has been supported by the Grant MTA-BME Lendület LP2021-06/2021 "Theory of new generation steel bridges" program of the Hungarian Academy of Sciences. The project supported by the Doctoral Excellence Fellowship Programme (DCEP) is funded by the National Research Development and Innovation Fund of the Ministry of Culture and Innovation and the Budapest University of Technology and Economics, under a grant agreement with the National Research, Development and Innovation Office.

References

[1] Xu, D.; Wang, Y.; Liu, X.; Chen, B.; Liu, M. (2023) *Local buckling behaviour of welded I-section steel stub columns with longitudinally profiled steel plates under axial compression: Testing , modelling and design*. Journal of Construsctional Steel Research 203, p. 107847, doi: 10.1016/j.jcsr.2023.107847.

[2] Yun, X.; Zhu, Y., Meng, X.; Gardner, L. (2023) *Welded steel I-section columns: Residual stresses, testing, simulation and design*. Engineering Structures 282, p. 115631, doi: 10.1016/j.engstruct.2023.115631.

[3] Su, A.; Sun, Y.; Liang, Y.; Zhao, O. (2021) *Experimental and numerical studies of S960 ultra-high strength steel welded I-sections under combined compression and minor-axis bending.* Engineering Structures 243, p. 112675, doi: 10.1016/j.engstruct.2021.112675.

[4] Lebastard, M.; Couchaux, M.; Bureau, A.; Hjiaj, M. (2023) *Impact of the fabrication process on the lateral–torsional buckling of welded I-section beams.* Thin-Walled Structures 188, p. 110761, doi: 10.1016/j.tws.2023.110761.

[5] Nascimento, S.; Pedro, J.J.O.; Santos, R.; Kuhlmann, U. (2023) *Experimental behaviour of plate girders in steel – Internal forces in intermediate transverse stiffeners.* Engineering Structures 291, p. 116425, doi: 10.1016/j.engstruct.2023.116425.

[6] Tankova, T. (2018) *Stability Design of Steel Columns, Beams and Beam-Columns: Behaviour, General Formulation and Reliability*. PhD thesis, University of Coimbra.

[7] Schaper, L.; Jörg, F.; Winkler, R.; Kuhlmann, U.; Knobloch, M. (2019) *The simplified method of the equivalent compression flange: Development based on LTB tests and residual stress measurements.* Steel Construction 12(4), pp. 264–277, doi: 10.1002/stco.201900033.

[8] Lebastard, M.; Kollár, D.; Horváth, A.; Bureau, A.; Couchaux, M.; Kövesdi, B. (2025) *Influence of flange fabrication process on residual stresses of welded I-section members*, Thin-Walled Structures, p. 114424, doi: 10.1016/j.tws.2025.114424 (under publication).

[9] MATLAB. version 9.9.0.1453 (R2024a). Natick, Massachusetts, USA: The Mathworks Inc.

[10] EN 1090-2:2018. Execution of steel structures and aluminium structures - Part 2: Technical requirements for steel structures.

[11] EN 1993-1-14:2020. Eurocode 3: Design of steel structures, Part 1-14: Design assisted by Finite element analysis.